THE GAMMA-RAY IRRADIATION SENSITIVITY AND DOSIMETRIC INFORMATION INSTABILITY OF RADFET DOSIMETER

by

Milić M. PEJOVIĆ

Faculty of Electronic Engineering, University of Niš, Niš, Serbia

Scientific paper
DOI: 10.2298/NTRP1304415P

The gamma-ray irradiation sensitivity to radiation dose range from 0.5 Gy to 5 Gy and post-irradiation annealing at room and elevated temperatures have been studied for p-channel metal-oxide-semiconductor field effect transistors (also known as radiation sensitive field effect transistors or pMOS dosimeters) with gate oxide thicknesses of 400 nm and 1 µm. The gate biases during the irradiation were 0 and 5 V and 5 V during the annealing. The radiation and the post-irradiation sensitivity were followed by measuring the threshold voltage shift, which was determined by using transfer characteristics in saturation and reader circuit characteristics. The dependence of threshold voltage shift ΔV_T on absorbed radiation dose *D* and annealing time was assessed. The results show that there is a linear dependence between V_T and *D* during irradiation, so that the sensitivity can be defined as V_T/D for the investigated dose interval. The annealing of irradiated metal-oxide-semiconductor field effect transistors at different temperatures ranging from room temperature up to 150 °C was performed to monitor the dosimetric information loss. The results indicated that the dosimeters information is saved up to 600 hours at room temperature, whereas the annealing at 150 °C leads to the complete loss of dosimetric information in the same period of time. The mechanisms responsible for the threshold voltage shift during the irradiation and the later annealing have been discussed also.

Key words: RADFET, absorbed radiation dose, gamma irradiation, threshold voltage, annealing

INTRODUCTION

It is well known that the ionizing radiation leads to the degradation of electrical characteristics of many electronic components and materials [1-4]. A special attention is focused on metal-oxide-semiconductor field-effect transistors (MOSFET) [4]. It was shown that such radiation leads to degradation of some electrical characteristics such as threshold voltage, leakage current, and breakdown voltage. Due to this fact, intensive investigations have been conducted in order to obtain MOSFET resistant to gamma irradiation. On the other hand, MOSFET sensitive to ionizing radiation have been developed in order to use them in dosimetric applications. Most commonly used are radiation sensitive p-channel MOSFET, also known as RADFET (which is an acronym for RADiation sensitive Field Effect Transistors [5]) as dosimeter have been used in space technology [6], in modern aircrafts [7, 8] in nuclear industry [9], in military [10, 11] in radiation therapy [12-14], and in radiology [15-17]. The major advantage of the RADFET as dosimeter is that the radiation-sensitive region, the oxide film, is very small [18, 19]. The sensing volume is much smaller than competing integral dose measuring devices, such as the ionizing chamber, the semiconductor diode or the thermoluminescent dosimeter (TLD). The smallest available liquid ionization chamber has sensing volume of about 2 mm^3, TLD volume is about 1 mm^3, while the semiconductor diode sensitive volume is about 0.3 mm^3 [19]. The RADFET sensitive volume is typical 1 µm 200 µm 200 µm. Attention is thus being turned to the use of RADFET especially where the dosimeter has to be inserted into a confined space, such as catheter [20, 21]. Also, the RADFET advantages include an immediate, nondestructive readout of information on the absorbed dose, a very low power consumption and very competitive price. The RADFET disadvantages are the need for calibration in different radiation fields, a relatively low resolution (starting about 10^{-2} Gy), and the non-reusability. The RADFET cannot be used for the subsequent determination of ionization dose. Namely, these dosimeters are only used to measure the maximum dose, which is determined by the type and sensitivity of RADFET. When it reaches the maximum radiation dose, these

---

* Corresponding author; e-mail: milic.pejovic@elfak.ni.ac.rs

dosimeters should be replaced. Our recent investigations [22, 23] have shown that these dosimeters can be recovered at room and elevated temperature for further measurements of gamma ray irradiation. The sensitivity of RADFET depends on the gate oxide thickness [24, 25], the gate oxide processing [26, 27], the value of gate bias during the irradiation [25], and the dose received by the RADFET [28].

The concept of RADFET is based on the build-up of positive oxide charge in the gate region when exposed to ionizing radiation. The electrical signal used as a dosimetric parameter is the threshold voltage. This parameter exhibits a shift when RADFET is irradiated. The basic mechanisms responsible for threshold voltage shift have previously been discussed [29-31]. It is shown that their behavior is a consequence of following processes: (1) the electron-hole pair generation, (2) the electron-hole recombination, (3) the hole transport, (4) the deep hole trapping, and (5) the radiation-induced interface and oxide traps formation. Beside the significant charge of threshold voltage during the irradiation, the RADFET mast has insignificant recovery after radiation (the long-term stability at room temperature), *i. e.*, the information about absorbed radiation dose mast be saved.

The aim of this work was to study RADFET sensitivity to gamma-ray irradiation with and without gate bias during irradiation. The annealing of these RADFET at room and elevated temperature has also been investigated in order to track the dosimetric information for a long time period. The mechanisms responsible for the threshold voltage shift during the irradiation and the threshold voltage shift of irradiated RADFET at room and elevated temperatures were also investigated.

EXPERIMENTAL DETAILS

The experimental samples were specially designed – the Al-gate p-channel enhanced MOSFET (RADFET) sensitive to gamma-ray irradiation. The samples were manufactured by Tyndall National Institute, Cork, Ireland. The gate oxides thicknesses of 400 nm and 1 μm, respectively, were grown at 1000 °C in dry oxygen and annealed for 15 min at 1000 °C in nitrogen. The post-metallization anneal was performed at 440 °C in forming gas for 60 min (a detailed description of these components can be found on http://web.tyndall.ie/projects/radfets). Figure 1 shows a single layout used in our experiments. The size of the chip is 1 mm 1 mm. There are total of four transistors (R1, R2, R3, and R4) on a single chip. Two of them have channel width and length of 300 μm and 50 μm, respectively (R1 and R3), while other two have channel width and length of 690 μm and 15 μm (R2 and R4). The RADFET R1 and R2 are regular four terminal devices with bulk, gate, drain and source terminals. The RADFET R3 and R4 have their gates and drains joint together as well as their bulks and sources and thus they are two terminal devices and they can easily be used in reader circuit configuration (see below). The chip also contains a diode, but it is irrelevant to the work described in this paper.

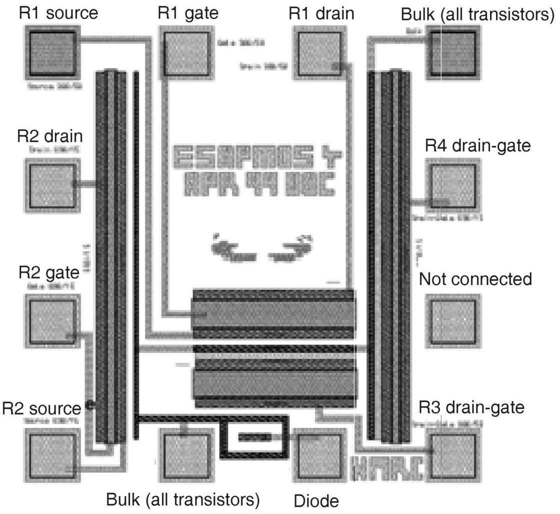

Figure 1. The single chip layout used in this study

The RADFET samples were irradiated using ^{60}Co beam in the range of absorbed radiation doses from 0.5 Gy to 5 Gy at absorbed radiation dose rate 0.02 Gy(Si)s^{-1}. The irradiation was performed in the Secondary Standard Dosimetry Laboratory of the Vinča Institute of Nuclear Sciences, Belgrade, Serbia. All measurements were conducted in a climate controlled laboratory environment with an ambient temperature of 20 0.2 °C. The air kerma rate at the reference point was measured with a calibrated vented 0.6 cm^3 ionization chamber (Model 30012, PTW, Freiburg, Germany) and electrometer Unidos (PTW, Freiburg, Germany). The calibration of the chamber in terms of air kerma and absorbed dose to water in the ^{60}Co beam quality had been performed at the Secondary Standards Dosimetry Laboratory of the International Atomic Energy Agency (Vienna, Austria). The calibration constants obtained in this way were traceable to BIPM. The values obtained were converted to the absorbed doses to for relevant material. The samples were irradiated without the bias on the gate (all terminals were grounded) and also with the voltage on the gate $V_{\mathrm{irr}} = 5$ V.

After irradiating to radiation dose of 5 Gy we performed an annealing of RADFET at different temperatures. Namely, the samples were divided into three groups for each thickness. The first group was annealed at room temperature, the second group was annealed at 100 °C, while the third was annealed at 150 °C using the Heraeus HEP2 system of temperature chambers. The gate voltage for all the samples during annealing was $V_{\mathrm{ann}} = 5$ V.

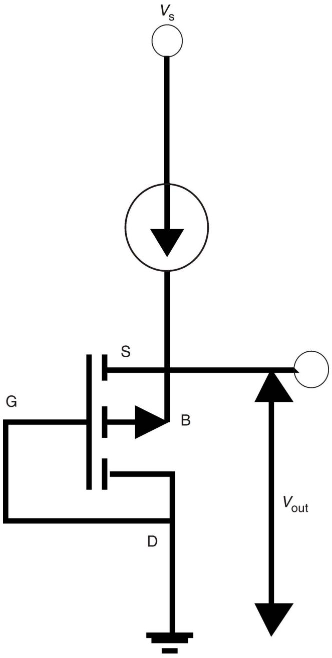

Figure 2. The reader circuit configuration for the threshold voltage measurement

The threshold voltage during irradiation and annealing was determined from transfer characteristics $(I_D)^{1/2} - V_G$ curve. The threshold voltage shift V_T can be expressed as $V_T = V_T - V_{T0}$, where V_{T0} is the threshold voltage before irradiation and V_T is the threshold voltage after irradiation. During the annealing V_T is the threshold voltage after certain annealing time.

Determining the threshold voltage from the transfer characteristics helps analyze physical processes in RADFET during the irradiation and the subsequent annealing. However, it would be very difficult to produce a stand-alone instrument that could provide a fast and accurate dose readout using this method. Taking this into consideration, additional experiments were performed where threshold voltage was determined using RADFET in so-called reader circuit configuration. Figure 2 shows electronic scheme for reader circuit measurement.

In this configuration, the gate and the drain are connected together, as well as the bulk and the source. In this arrangement, a RADFET is treated as the two terminals device. A constant current is forced in the bulk-source connection, while the gate-drain connection is grounded. The voltage values obtained for 10 μA were used to determine the threshold voltage shift. This value of the current was selected because it was close to the zero temperature coefficients for our RADFET. Namely, when reader circuit characteristics are measured at different temperatures, all of them intersect for current value of approximately 10 μA. So, the V_T readout at 10 μA is independent of the temperature.

The transfer and the reader circuit characteristics were performed by Keithley 4200 Semiconductor Characterization System (SCS). This system is equipped with three medium-power source measuring units (4200 SMU). The source measuring units have four voltage ranges (200 mV, 2 V, 20 V, and 200 V) and three current regions (100 μA, 100 mA, and 1 A). One of the source-measuring units is equipped with a preamplifier for measuring very small current (in the order 1 pA).

RESULTS AND DISCUSSION

Figure 3 shows the threshold voltage shift ΔV_T as a function of the absorbed dose D obtained using transfer characteristics in saturation and reader circuit characteristics of RADFET with gate oxide thicknesses of 400 nm and 1 μm when all terminals were grounded during irradiation ($V_{irr} = 0$). The agreement between values of ΔV_T obtained from transfer characteristics in saturation and reader circuit measurements is satisfactory (within 1%), justifying the use of reader circuit configuration in practical applications. Figure 4 represents also the dependence as shown in fig. 3, but in the case when gate bias during irradiation was $V_{irr} = 5$ V.

According to the results shown in figs. 3 and 4 it can be noted that the increase in gate oxide thickness or in voltage at the gate leads to the increase in sensitivity of RADFET.

The dependence between the V_T and D can be expressed as $V_T = AD^n$ [32], where A is the constant and n is the degree of linearity. Ideally, this dependence is linear, *i. e.* $n = 1$, where A represents the sensitivity V_T/D. The symbols in figs. 3 and 4 represent experimental values while the solid lines are determined by fitting the data with expression $V_T = AD^n$ for $n = 1$. For RADFET with 400 nm and 1 μm gate oxide thicknesses irradiated with no gate bias (fig. 3), the values of fitting correlation factors are 0.9981 and

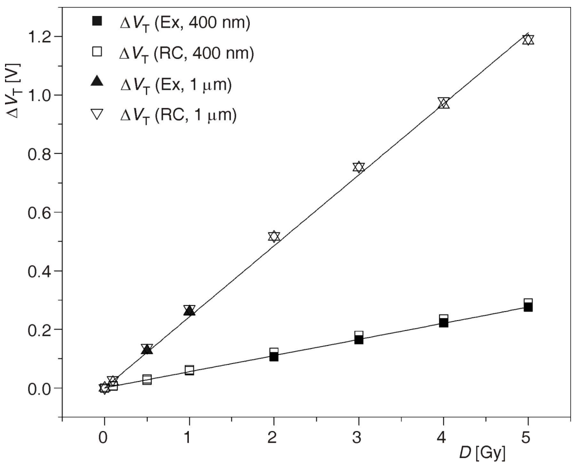

Figure 3. Threshold voltage shift ΔV_T determined using reader circuit (RC) and extrapolated $(I_D)^{1/2} - V_G$ (Ex) without gate bias during irradiation (V_{irr} = 0 V) for RADFET with 400 nm and 1 μm gate oxide thickness

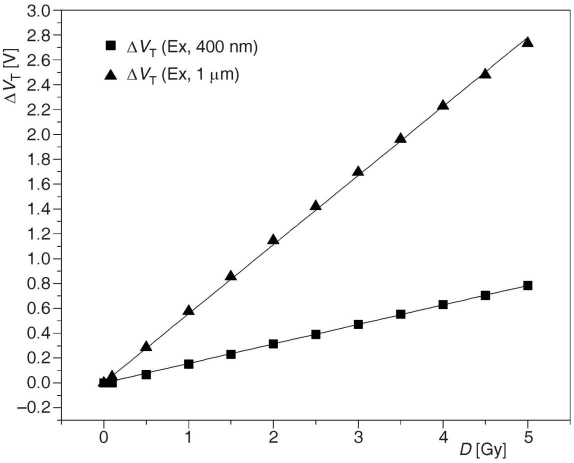

Figure 4. The threshold voltage shift ΔV_T determined by using the extrapolated $(I_D)^{1/2}$ – V_G (Ex) curve for RADFET with 400 nm and 1 μm gate oxide thickness; the gate bias during irradiation was V_{irr} = 5 V

0.99943, respectively. For RADFET with 400 nm and 1 μm gate oxide thicknesses irradiated when gate bias was 5 V (fig. 4), the values of fitting correlation factors are 0.99947 and 0.9993, respectively. Because the linear fitting coefficients are very close to one, it can be assumed that there is a linear dependence between the V_T and D, that the sensitivity of RADFET is the same for the dose interval from 0.5 to 5 Gy, and that it can be expressed as V_T/D.

Our recent investigations [32] for RADFET used in this paper have shown that the positive oxide traps in the oxide contributions to the threshold voltage shift V_T is dominant. During the irradiation, the density of positive oxide traps is for more than order of magnitude higher than the interface traps density (traps at Si/SiO$_2$ interface also known as true interface traps). Because of that, the further analysis of mechanisms influencing V_T during the irradiation and annealing will be focused only on the presence of positive oxide traps. The increase of V_T value during the irradiation can be most readily explained on the basis of previously proposed model [33-35]. The crucial role in this model belongs to the E_γ center, which is a weak Si-Si bond in the oxide caused by an oxygen atom vacancy between two Si atoms, each back bounded to three oxygen atoms [36]. The E_γ center acts as a hole trap and they are located exclusively in the oxide (fixed traps) and near the Si/SiO$_2$ interface (switching traps). The fixed traps are E_γ centers and hence incapable of exchanging charge with Si during the time frame of the measurements, while switching traps are capable of exchanging the charge with Si within the measurement time frame.

The number of created positive oxide charge rises with the number of holes which have avoided recombination with electrons. For V_{irr} = 0 V (fig. 3), the electric field in the oxide is only a consequence of the work function difference between the gate and the substrate (the zero-bias conditions are equal to the gate bias of 0.3 V), so the probability for electron-hole recombination is higher than in the case V_{irr} = 5 V. Namely, for V_{irr} = 5 V the large number of holes will escape the initial recombination than in the case when V_{irr} = 0, which further increases the probability for their capture at E_γ centers and consequently increase positive oxide charge. Such a conclusion is in agreement with the results presented in figs. 3 and 4. However, in thicker oxides for the same irradiation dose a larger number of E_γ centers is being created, which is also in agreement with the results presented in figs. 3 and 4.

Figures 5 and 6 show the threshold voltage shift V_T during the annealing of RADFET with gate oxide thickness of 400 nm which were previously irradiated without gate bias (V_{irr} = 0) and gate bias of V_{irr} = 5 V,

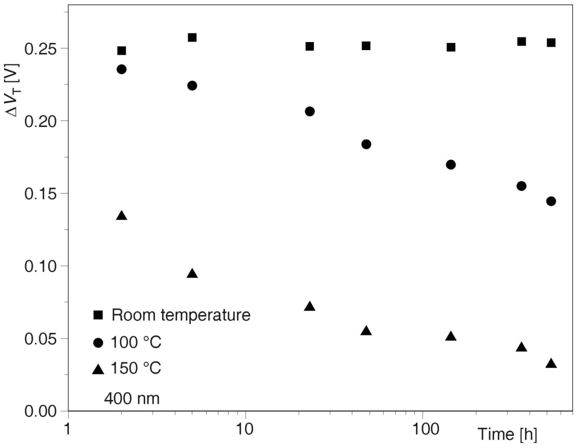

Figure 5. The threshold voltage shift ΔV_T during the annealing at room temperature at 100 °C and 150 °C for RADFET with 400 nm gate oxide thickness; during irradiation gate bias was V_{irr} = 0 V and gate bias during annealing was V_{ann} = 5 V

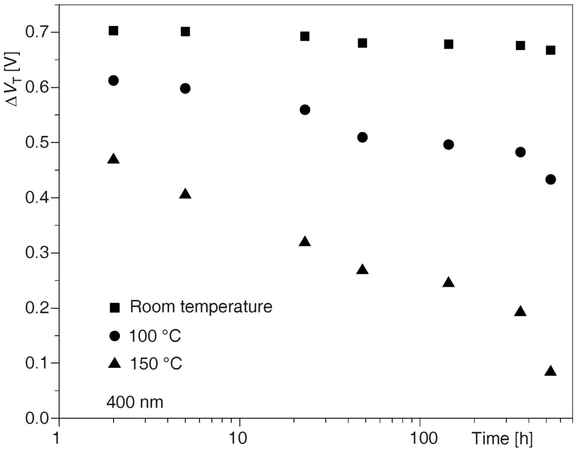

Figure 6. The threshold voltage shift ΔV_T during annealing at room temperature at 100 °C and 150 °C for RADFET with 400 nm gate oxide thickness; during the irradiation, gate bias was V_{irr} = 5 V and the gate bias during the annealing was V_{ann} = 5 V

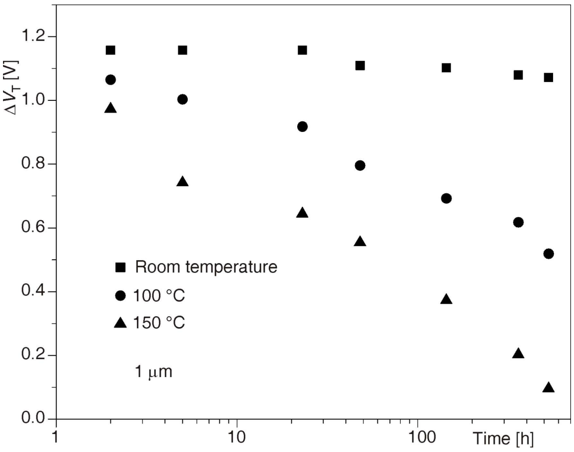

Figure 7. The threshold voltage shift ΔV_T during the annealing at room temperature at 100 °C and 150 °C for RADFET with 1 μm gate oxide thickness; during the irradiation gate bias was $V_{irr} = 0$ V and the gate bias during the annealing was $V_{ann} = 5$ V

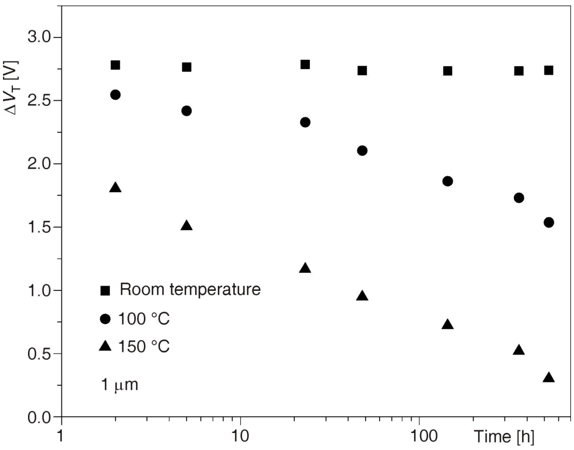

Figure 8. The threshold voltage shift ΔV_T during the annealing at room temperature at 100 °C and 150 °C for RADFET with 1 μm gate oxide thickness; during the irradiation, the gate bias was $V_{irr} = 5$ V and the gate bias during the annealing was $V_{ann} = 5$ V

respectively. Figures 7 and 8 represent the same dependence for RADFET with 1 μm gate oxide thickness. The annealing process for these samples was performed at room temperature, at 100 °C, and at 150 °C with gate bias of $V_{ann} = 5$ V, while the total annealing time was 600 hours. It can be seen that the V_T changes insignificantly during annealing at room temperature, *i. e.* the information on the absorbed dose is saved. The increase in temperature during annealing decreases V_T values, so annealing at 150 °C decreases the value of V_T which is close to zero for annealing time of 600 hours. This shows that at this temperature the information on the absorbed dose is completely lost. Such behavior is in a good agreement with our recently published results [22, 23] that these components can undergo full recovery and therefore can be reused in dosimetric applications.

The decrease of ΔV_T during the annealing at elevated temperatures (figs. 5-8), *i. e.* the loss of information on the absorbed dose is mostly due to the decrease of positive oxide trapped charge formed by the capture of holes at E_γ centers. Namely, the decrease in the positive oxide charge density, formed by irradiation, during annealing can be caused by field-assisted and thermal-assisted emission of electrons from silicon [37-39] as well as thermal-assisted emission of electrons from valence bands of the oxide [39]. It is presumed [40] that there are three energy levels in the band gap oxide which holds the positive charge radiation defects which make the positive trapped charge and which make traps centers of electrons. One energy level can be found in the area of the conductive band of the substrate (E_1), the second in the area of the valence band of the substrate (E_2) and the third above the top of the valence band of the oxide (E_3). The electrons which tunnel from the substrate, or which are thermally emitted from the valence band of the oxide, can get trapped at these trapping centers, thus neutralizing/compensating them, leading to the decrease of positive oxide charge. The occupancy of the E_1 level (number of positive charge defects on this level) depends on the temperature and positive bias on the gate. Namely, in case of higher temperature there are a larger number of electrons in the conductive band substrate, so a larger number of electrons can tunnel to the trapping centers at that level. Because of this, with the increase in positive polarization of the gate the height of the potential tunneling barrier decreases, which increases the probability of electron tunneling at the energy level E_1. The occupancy of the E_2 level is almost independent on the annealing temperature; however, it is highly dependent on the value of the positive bias on the gate (voltage increase leads to the height decrease of the potential tunneling barrier and increase in number of electrons at the valence band substrate near Si/SiO_2). The occupancy of the E_3 level does not depend on the gate voltage; however, it is highly dependent on temperature (with the temperature increase, increases the number of electrons which can leave the valence band of the oxide).

Since the change in V_T during the annealing at room temperature is very small (figs. 5-8) it can be concluded that neither field-assisted nor thermal-assisted emission of electrons from the oxide or silicon have a significant impact on the neutralization/compensation of positive oxide charge. Namely, the room temperature and the gate voltage $V_{ann} = 5$ V do not activate energy levels E_1, E_2, and E_3. As a consequence, the information about the absorbed dose is practically saved up to 600 hours after irradiation. During the annealing at temperatures of 100 °C and 150 °C the, values of V_T decrease, *i. e.* the loss of information about absorbed dose occurs. Moreover, the annealing at 150 °C in duration of 600 hours leads to the complete loss of information on absorbed dose. This behavior of V_T values at elevated temperatures is a consequence of the neutralization/compensation of the positive oxide trapped charge due to the thermal-assisted emission of electrons from the conductive band of the silicon and the valence band of the oxide (energy levels E_1 and E_3 are activated).

CONCLUSIONS

The paper presents irradiation (for gamma-ray irradiation doses to 5 Gy) and post irradiation (at room and elevated temperature) sensitivity of Al-gate RADFET with oxide thicknesses of 400 nm and 1 μm. The sensitivity was followed on the basis of the threshold voltage shift V_T as a function of the absorbed dose D and the annealing time. The results show that there is approximately a linear dependence between V_T and D, so that the sensitivity can be defined as V_T/D for the investigated dose interval. After the irradiation dose information is stored at room temperature for up to 600 hours, which presents their main advantage in comparison to other dosimeters which are used in practical purposes. However, the dosimetric information can be completely erased by heating the irradiated RADFET for a long time period. By analyzing physical processes which are responsible for the change in the threshold voltage shift during the irradiation of RADFET, it was concluded that E_γ centers, which are formed during the irradiation, play the main role. These centers represent hole traps responsible for the increase of positive oxide charge during the irradiation. Their density increases with the increase of the oxide thickness and the gate bias. An insignificant change in the value of V_T, *i. e.* preserving the information about the absorbed dose at room temperature is a consequence of field-assisted and thermal-assisted emission of the electrons from silicon as well as the thermal-assisted emission of electrons from the valence band of the oxide, having no significant effect on the neutralization/compensation of positive oxide trapped charge. At elevated temperature, thermal-assisted emission of electrons from silicon and from the valence band of the oxide play a significant role in the neutralization/compensation of positive oxide trapped charge which thus leads to the loss of the dosimetric information. The recovery at 150 °C for the time of 600 hours leads to the complete loss of dosimetric information ($V_T = 0$) that allows components' reusability in dosimetric applications.

ACKNOWLEDGEMENT

The Ministry of Education, Science and Technological Development of the Republic of Serbia, supported this work financially through the project No. 17007.

REFERENCES

[1] Vujisić, M., *et al*., Radiation Hardness of COT EPROM and E^{2}PROM, *Radiation Effects and Deffects in Solids: Incorporating Plasma Science and Plasma Technol., 165* (2010), 5, pp. 362-369

[2] Lazarević, Dj. R., *et al*., Radiation Hardness of Indium Oxide Films in the Copper-Pair Insulator State, *Nucl Technol Radiat, 27* (2012), 1, pp. 40-43

[3] Stanković, S. J., *et al*., MSV Signal Processing System for Neutron-Gamma Discrimination in a Mixed Field, *Nucl Technol Radiat, 27* (2012), 2, pp. 165-170

[4] ***, Current Topics in Ionizing Radiation Research, Ed., M. Nenoi, InTech, Rijeka, Croatia, 2012

[5] Hughes, R., Theory of Response of Radiation Sensing Field-Effect Transistors, *J. Appl. Phys., 58* (1985), 3, pp. 1375-1380

[6] Holmes-Siedle, A., The Space-Charge Dosimeter-General Principles at a New Method of Radiation Detection, *Nucl. Instrum. Methods, 121* (1974), 1, pp. 169-179

[7] Ward, A. K., *et al*., The Meteosat-P2 Radiation Effects Experiment, *Proceedings*, 40th Congress of International Astronautical Federation, Malaga, Spain, 1989, pp. 151-159

[8] Adams, L., *et al*., Measurements of SEU and Total Dose in Geostationary Orbit under Normal and Solar Flare Conditions, *IEEE Trans. Nucl. Sci., 38* (1991), 6, pp. 1686-1692

[9] Leffler, J. S, Lingrern, S. R, Holmes-Siedle, A. G., Applications of RADFET Dosimeters to Equipment Radiation Qualification and Monitoring, *Trans. of American Nucl. Society, 60* (1989), 1, pp. 533-536

[10] August, L. S., Desing Criteria for a High-Dose MOS Dosimeter for Use in Space, *IEEE Trans. Nucl. Sci., 31* (1984), 1, pp. 801-803

[11] August, L. S., Curcle, R. R., Advantages of Using of PMOS FEt Dosimeter In High-Dose Radiation Effects Testing, *IEEE Trans. Nucl. Sci., 31* (1984), 6, pp. 1113-1115

[12] Chuang, C. F., Verley, L. J., Xia, P., Investigation of the Use of MOSFET for Clinical IMRT Dosimetric Verification, *Med. Phys., 29* (2002), 6, pp. 1109-1115

[13] Jornet, N., *et al*., Comparison Study of MOSFET Detector and Diodes for Entrace *in vivo* Dosimetry in 18 MV X-Ray Beam, *Med. Phys., 31* (2004), 9, pp. 2534-2542

[14] Lavallee, M. C., Gingras, L., Beaulieu, L., Energy and Integrated Dose Dependence of MOSFET Dosimeter Sensitivity for Irraiation Energies Between 30 kV and ^{60}Co, *Med. Phys., 33* (2006), 10, pp. 3682-3689

[15] Brower, M. V., Hitenlang, D. E., The Characterization of a Commercial MOSFET Dosimeter System for Use in Diagnostic X-Ray, *Health Phys., 75* (1998), 2, pp. 197-204

[16] Pomije, B. D., *et al*., Comparison of Angular Free-In-Air Tissue-Equivalent Photon Response Measurements in p-MOSFET Dosimeters, *Health Phys., 80* (2000), 5, pp. 497-505

[17] Dong, S. L., *et al*., Characterization of High-Sensitivity Metal-Oxide-Semiconductor Field Effect Transistor Dosimeters System and LiF: Mg, Cu, P Thermoluminescence Dosimeters for Use in Diagnostic Radiotherapy, *Appl. Radiat. Isot., 57* (2002), 6, pp. 883-891

[18] Rosenfeld, A. B., *et al*., MOSFET Dosimeter: Role of Encapsulation on Dosimetric Characteristics in Mixed Gamma-Neutron and Megavoltage X-Ray Field, *IEEE Trans. Nucl. Sci., 42* (1995), 6, pp. 1870-1877

[19] Dasu, A., Lofroth, P.-O., Wickman, G., Liquid Ionization Chamer Measuremnt of Dose Distribution in

Small 6 MV Photon Beam, *Phys. Med. Biol., 43* (1998), 1, pp. 21-36

[20] Huges, R. C., *et al*., Miniature Radiation Dosimeter for *in vivo* Radiation Measurements, *Int. J. Radiat. Oncol. Biol. Phys., 14* (1988), 5, pp. 963-967

[21] Gladstone, D. J., *et al*., A Miniature MOSFET Radiation Dosimeter Probe, *Med. Phys., 21* (1994), 1, pp. 1721-1728

[22] Pejović, M. M., *et al*., Succesive Gamma-Ray Irradiation and Corresponding Post-Irradiation Annealing of pMOS Dosimeters, *Nucl Technol Radiat, 27* (2012), 4, pp. 341-345

[23] Pejović, M. M., Pejović, M. M, Jakšić, A. B., Response of pMOS Dosimeters on Gamma-Ray Irradiation During its Reuse, *Radiation Protection Dosimetry, 155* (2013), pp. 394-403

[24] Holmes-Siedle, A., Adams, A., RADFET: A Review of the Use of Metal-Oxide-Silicon Devices as Integrating Dosimeters, *Radiation Physycs and Chemistry, 28* (1986), 2, pp. 235-244

[25] Sarrabayrouse, G., Bellaouar, A., Rossel, P., Electrical Properties of MOS Radiation Dosimeters, *Revue Phys. Appl., 21* (1986), 4, pp. 283-287

[26] Aubuchon, K. G., Radiation Harding of p-MOS Devices by Optimization of the Thermal SiO_2 Gate Insulator, *IEEE Trans. Nucl. Sci., 18* (1971), 1, pp. 117-121

[27] Derbenwick, G. F., Gregory, B. L., Process Optimization of Radion/Hardned CMOS Integrated Circuit, *IEEE Trans. Nucl. Sci., 22* (1975), 6, 2151-2156

[28] Pejović, S, Characteristics of a pMOSFET Suitable for Use in Radiotherapy, *Appl. Radiation and Isotopes, 77* (2013), 1, pp. 44-49

[29] Soubra, M., Cygler, J., Maskay, G., Evaluation of a Dual Bias Metal-Oxide-Silicon-Semiconductor Field Effect Transistors Detector as Radiation Dosimeter, *Med. Phys., 21* (1994), 1, pp. 567-572

[30] Benedetto, J. M., Boesch, H. E., McLean, F. B., Dose Energy Dependence of Interface Trap Formation in ^{60}Co and X-Ray Environments, *IEEE Trans. Nucl. Sci., 35* (1988), 6, pp. 1260-1264

[31] Oldham, T. R., McLean, F. B., Total Ionizing Dose Effect in Mos Oxides and Devices, *IEEE Trans. Nucl. Sci., 50* (2003), 6, pp. 483-499

[32] Pejović, M. M., Pejović, M. M., Jakšić, A. B., Contribution of Fixed Oxide Traps to Sensitivity of pMOS Dosimeters During Gamma Ray Irradiation and Annealing at Room and Elevated Temperature, *Sensors and Actuators A, 174* (2012), pp. 85-90

[33] Lelis, A. L., *et al*., Reversibility of Trapped Hole Annealing, *IEEE Trans. Nucl. Sci., 35* (1988), 6, pp. 1186-1191

[34] Lelis, A. L., *et al*., The Nature of Trapped Hole Annealing Process, *IEEE Trans. Nucl. Sci., 36* (1989), 6, pp. 1808-1815

[35] Lelis, A. L., Oldham, T. R., Time Dependence of Switching Oxide Traps, *IEEE Trans. Nucl. Sci., 41* (1994), 6, pp. 1835-1843

[36] Feigl, F. J., Fowler, W. B., Yip, K. L., Oxygen Vacancy Model for the Center in SiO_2, *Solid State Commun., 14* (1974), 3, pp. 225-229

[37] Lenahan, P. M., Dressendorfer, P. V., Hole Traps and Trivalent Silicon Centers in Metal/Oxide/Silicon Devices, *J. Appl. Phys., 55* (1984), 10, pp. 3495-3499

[38] Oldham, T. R., Lelis, A. L., McLean, F. B., Spatial Dependence of Trapped Holes Determined from Tunneling Analysis and Measured Annealing, *IEEE Trans. Nucl. Sci., 37* (1986), 6, pp. 1203-1210

[39] McWhorter, P. J., Miller, S. L., Miller, W. M., Modeling the Anneal of Radiation-Induced Trapped Holes in a Varying Thermal Environment, *IEEE Trans. Nucl. Sci., 37* (1990), 6, pp. 1682-1689

[40] Schwank, J. R., *et al*., Physical Mechanisms Contributing To Devices “Rebound”, *IEEE Trans. Nucl. Sci., 31* (1984), 6, pp. 1434-1438

Received on August 23, 2013
Accepted on November 27, 2013

Милић М. ПЕЈОВИЋ

ОСЕТЉИВОСТ И НЕСТАБИЛНОСТ ДОЗИМЕТРИЈСКЕ ИНФОРМАЦИЈЕ RADFET ДОЗИМЕТАРА ОЗРАЧИВАНИХ ГАМА ЗРАЧЕЊЕМ

Истраживана је осетљивост p-каналних MOSFET-ова са дебљином оксида од 400 nm и 1 μm (такође познатих као RADFER или pMOS дозиметри) на гама зрачење за опсег доза од 0.5 Gy до 5 Gy, као и њихов опоравак на собним и повишеним температурама. Поларизације на гејту током зрачења биле су 0 V и 5 V, док је током опоравка износила 5 V. Осетљивост током зрачења и опоравка је праћена на основу промена напона прага који је одређиван из преносних карактеристика у сатурацији и методом једне тачке. Праћена је промена напона прага ΔV_T у зависности од дозе D и времена опоравка. Резултати показују да постоји линеарна зависност између ΔV_T и D тако да се осетљивост може дефинисати као $\Delta V_T/D$ за истраживани интервал доза. Опоравак озрачених RADFET-а на различитим температурама почев од собне до 150 °C је вршен ради праћења губитка дозиметријске информације о апсорбованој дози. Резултати показују да се информација о апсорбованој дози на собној температури одржава до 600 часова, док се на температури од 150 °C у потпуности губи за исто време. Механизми одговорни за промену напона прага током озрачивања и каснијег опоравка такође су разматрани.

Кључне речи: RADFET, апсорбована доза, гама зрачење, напон прага, опоравак